www.ptcer.pl/mccm

MATERIAŁY CERAMICZNE /CERAMIC MATERIALS/, 65, 2, (2013), 227-234

Effects of the nickel oxalate precursor and SPS consolidation process on properties of Ni/Al_2O_3 composites

Agata Golonka*, Ewa Drożdż-Cieśla, Norbert Moskała, Waldemar Pyda

AGH University of Science and Technology, Faculty of Material Science and Ceramics
al. A. Mickiewicza 30, 30-059 Kraków, Poland
*e-mail: ahg@agh.edu.pl

Abstract

A precipitation-calcination method based on nickel oxalate reduction was used to obtain nickel nanoparticles dispersed within alumina powder. The powder was SPS consolidated to manufacture Ni/Al_2O_3 composites, containing a nickel additive of 1.7 vol.% and 10 vol.%. Two ways of incorporation of the nickel oxalate particles into the alumina powder were applied: (i) attrition milling assisted dispersion of a mixture of the dried powder of precipitation derived nickel oxalate and the alumina one in ethanol, (ii) direct precipitation of nickel oxalate on alumina particles. The SPS sintering of the studied powders was carried out for 7 min at 1400 °C under a pressure of 20 MPa in an argon atmosphere with purity 5.0 (99.999%). XRD and TEM measurements were performed to characterize the phase composition and morphology of the powders, respectively. XRD, microstructural (SEM/EDS) and mechanical tests were carried out for sintered bodies. It has been stated that agglomerated nanoparticles of nickel oxalate were the precursor of nano-nickel in the studied Ni-alumina powders. The way of incorporation of the nickel oxalate precursor and SPS sintering influenced the microstructure and properties of the Ni/Al_2O_3 composites. The segregation of nickel enhanced with the SPS sintering has been detected in the composite microstructure. The Ni/Al_2O_3 composites showed increased hardness, fracture toughness and abrasive resistance when compared to alumina with no nickelic particles.

Keywords: Al_2O_3, Ni, Nickel oxalate, Microstructure - final, SPS

WPŁYW SZCZAWIANOWEGO PREKURSORA NIKLU I PROCESU KONSOLIDACJI SPS NA WŁAŚCIWOŚCI KOMPOZYTÓW Ni/Al_2O_3

Metoda strącania szczawianu niklu i jego prażenia w warunkach redukcyjnych została wykorzystana do otrzymania nanocząstek niklu rozproszonych w proszku tlenku glinu. Proszek ten konsolidowano za pomocą metody SPS, aby wytworzyć kompozyty Ni/Al_2O_3, zawierające 1,7% obj. i 10% obj. niklu. Zastosowano dwa sposoby wprowadzania cząstek szczawianu nikli: (1) rozpraszanie mieszaniny strąconego i wysuszonego proszku szczawianu niklu w proszku Al_2O_3, wspomagane mieleniem atrycyjnym w etanolu, (2) bezpośrednie strącanie szczawianu niklu na cząstkach tlenku glinu. Spiekanie SPS badanych proszków przeprowadzono w 1400 °C przez 7 min, stosując ciśnienie 20 MPa i atmosferę argonu o czystości 99,999%. Rentgenowską analizę fazową i mikroskopię transmisyjną wykorzystano do określenia odpowiednio składu fazowego i morfologii proszków. Rentgenowską analizę fazową, badania mikrostrukturalne metodą mikroskopii skaningowej połączonej z EDS i badania właściwości mechanicznych przeprowadzono w przypadku spieczonych materiałów. Stwierdzono, że zaglomerowane nanocząstki szczawianu niklu stanowiły prekursor nanocząstek niklu w badanych proszkach tlenku glinu. Mikrostruktura i właściwości kompozytów Ni/Al_2O_3 były zależne od sposobu wprowadzania prekursora szczawianowego i zastosowanej metody spiekania (SPS). Zaobserwowano segregację niklu w mikrostrukturze kompozytów, wzmocnioną spiekaniem w warunkach SPS. Kompozyty Ni/Al_2O_3 pokazały zwiększoną twardość, odporność na pękanie i odporność na zużycie ścierne w porównaniu z tlenkiem glinu bez wtrąceń niklowych.

Słowa kluczowe: Al_2O_3, Ni, szczawian niklu, mikrostruktura finalna, SPS

1. Introduction

Incorporating dispersed nickel particles to the alumina matrix improves mechanical properties and electrical conductivity as a result of composing the ductile and electrically conductive phase with the brittle and dielectric one [1-10]. The level of property improvement depends on chemical and phase composition [8-9, 11-13], and microstructural features such as content [1-12], shape [14], size [15] and location [16] of dispersed particles. Those features arise out of methods of preparation and processing precursor powders to the Ni/Al_2O_3 micro- and nanocomposites. Several methods have been developed, including a powder metallurgy technique [7-9, 13, 16-17], a selective reduction process [1], a powder coating process [3, 15, 18-19], a sol–gel process [2, 20-21], an electroless deposition process [12, 22], reduction of $NiAl_2O_4$ [23] and reactive hot pressing [5].

The fine scale homogeneity of dispersion of nickel particles into the alumina matrix, narrow size distribution of the particles and high relative density of the composites are required to achieve the efficient reinforcement. For the latter reason, pressure assisted sintering techniques have been preferred, especially hot pressing (HP) [e.g. 2, 5, 12] and spark plasma sintering (SPS or PECS – pulsed electric current sintering) [15, 18], and powder forming routs for pressureless sintering have been optimized [7, 24].

The nickel particle size effect, especially in the nanometric range, is an important issue in the mechanical properties of Ni/alumina composites. The decrease of the particle size in the composite may negatively affect toughness values due to restraining the effects of the "bridging mechanism" behind the crack front [10]. On the contrary, it may promote an increase in the strength as a consequence of the reduction of the critical flaw size.

The most remarkable effect of nano-nickel particles has been found on hardness of the Ni/alumina composites, coming from the synergic effect of nanometer size, clustering and ceramic/metal interface features [19]. Maximum hardness values of 25 GPa were measured for the SPS consolidated alumina composite with a 2.5 vol.% nano-Ni content, and the material showed an excellent wear behaviour. The nano-Ni coated powder was prepared by dispersion of colloidal alumina in the ethanol solution of nickel nitrite followed by calcination of the dried mixture at 400 °C for 2 h in air to obtain an Al_2O_3/NiO mixed powder which was heat treated at 500 °C for 2 h in a 90%Ar/10%H_2 atmosphere to reduce NiO to metallic Ni.

It must be noticed that the processing of nanometric powders at low temperatures and keeping the fine-grained microstructure after sintering at high temperatures present a lot of difficulties. Nanoparticles have very high susceptibility to create agglomerates, affecting their packing in a green body, and sintering is always accompanied by grain coarsening which increases easily the grain size over the nanoscale.

The research objective of the presented work was to obtain Ni/Al_2O_3 nano-composites by using a new composite powder preparation method based on employing nickel oxalate, and to explore effects of distribution of nickel particles in the microstructure on properties of the resultant nanocomposites. Special emphasis was focused on determination of hardness, fracture toughness and wear resistance of the Ni/Al_2O_3 composites, being the most important features of cutting tool materials for machining. The SPS method was used to consolidate the composite powders into dense and fine-grained materials.

2. Experimental procedure

Ni/Al_2O_3 composite materials containing 1.7 vol.% and 10 vol.% of nickel particles were obtained from α-Al_2O_3 powder (A16, Alcoa; Table1), showing a specific surface area of 10.85 m^2/g and an equivalent particle size of 139 nm. The nickel particles were incorporated into the alumina powder with a precipitation-calcination method using nickel oxalate as the precursor and a reducing atmosphere for heat treatment. Two variants of the method were applied, affecting homogeneity of distribution of the nickel particles in the resultant composite.

In both cases nickel oxalate powder, being a precursor of nickel particles, was obtained by using nickel(II) nitrite (a.p., Chempur) and oxalic acid (a.p., Chempur). The aqueous solution of oxalic acid (0.5 M) was always added dropwise to the solution or suspension containing nickel(II) nitrite (0.5 M) during intensive mixing, and aqueous ammonia adjusted the pH to 4.

In the case of the composite added with 1.7 vol.% of nickel particles (Al/1.7Ni), the deposit of nickel oxalate was first dried at 105 °C to the constant weight, and then incorporated to the alumina powder. The resultant mixture was homogenised for 1 h in anhydrous ethanol using a laboratory ball mill of the attritor type. 3Y-TZP grinding media (TOSOH) were used for milling.

Table 1. Chemical composition of studied composites.
Tabela 1. Skład chemiczny badanych kompozytów.

Description	Volumetric composition [vol.%]	Weight percent composition* [wt%]
Al/0Ni	100% α-Al_2O_3	100% α-Al_2O_3
Al/1.7Ni	98.3% α-Al_2O_3 and 1.7% Ni	96.4% α-Al_2O_3 and 3.6% Ni
Al/10Ni	90% α-Al_2O_3 and 10% Ni	78.2% α-Al_2O_3 and 21.8% Ni

* calculated assuming theoretical densities of Ni and α-Al_2O_3 to be 8.908 g/cm^3 and 3.99 g/cm^3, respectively.

In the case of the Al/10Ni composite, containing the 10 vol. % nickel additive, nickel oxalate was precipitated from nickel(II) nitrite and oxalic acid directly on the particles of alumina powder during intensive mixing of the system. Water was evaporated from the slurry at 105 °C to the constant weight of the mixture, and no additional milling was applied in subsequent processing of the powder.

Both composite mixtures were heated for 1 h at a temperature of 360 °C in the atmosphere of Ar + 10% H_2 to decompose nickel oxalate, and obtain metallic nickel. The low decomposition temperature was selected to produce nickel particles as small as possible, and keep consolidation of the nickel aggregates to a minimum. The reduction was carried out in a vacuum tube furnace with graphite heating elements.

In this study, spark plasma sintering (SPS) has been chosen to consolidate both the composite and pure alumina powders. The SPS consolidation was carried out by using a HP D5 machine made by FCT-System GmbH. The sintering was carried out for 7 min. at 1400 °C in the argon atmosphere of purity 5.0 (99.999 %). An external pressure of 20 MPa was applied to the powders during sintering.

The phase composition and microstructure of sinters were examined, basing on XRD and SEM measurements, respectively. Densities of the sinters were measured by means of the Archimedes' method.

The analysis of phase composition of the sinters was carried out by means of an X'Pert Pro diffractometer produced by PANalytical, and the Rietveld method. Monochromatic radiation with a wavelength of 0.1540598 nm corresponded to the emission Kα1 line of copper; an analysis step of 0.008° and a range of 20-90° in the 2θ scale were used. The XRD analysis delivered the phase composition of the composites together with the content of each phase detected.

The observation of morphology of the composite powders was carried out by means of a transmission electron microscope JEOL JEM1011 at a voltage of 100 kV. The sample of each powder was dispersed in anhydrous ethanol, and placed on a carbon thin film.

Examination of the microstructure of sintered bodies was carried out by means of a scanning electron microscope Nova NanoSEM230 produced by FEI Company. The

measurement was made in the low vacuum regime (LVD) using secondary electrons. The local point analysis of the chemical composition was carried out by means of energy dispersive spectroscopy (EDS) to identify the component phases. Before the observations, the samples were finally polished on polishing cloth damped in colloidal silica (SPU – Suspension, Struers) with the grain size of 1 μm.

The measurements of hardness and fracture toughness were carried out by means of a FV-700 apparatus produced by Futur-Tech from Japan. The Vickers indentation method was used. The measurement of hardness was carried out at a load of 9.807 N applied for 15 s. Ten indents were made for each sample. The measurement of fracture toughness was carried at a load of 98.7 N. A loading time for the indenter was set for 15 s.

Wear resistance of the studied materials was checked by the Dry Sand test. The test refers to the ASTM G 6585 standard. In this test, the volume of a material abraded by SiC grains is a measure of the wear resistance. This volume was determined from the difference between sample masses before and after the test, and apparent density of the material.

3. Results

3.1. Powder characteristics

Nanosized particles of nickel oxalate were precipitated on the surface of submicromeric in size alumina particles as shown in Fig. 1. The nickel oxalate primary particles ranged from 15 nm to 45 nm, and a large majority of them was agglomerated. The agglomerates showed sizes typically smaller than 100 nm, but bigger clusters also occurred. Distribution of the primary particles and the agglomerates of nickel oxalate among the alumina particles was not uniform. The alumina particles completely covered with nickel oxalate existed next to the separate big oxalate agglomerates and the alumina particles with surfaces containing a small amount of single primary nickel oxalate particles.

A mean crystallite size of 22 nm has been measured for nickel oxalate in the Al/10Ni powder, basing on the X-ray line broadening.

X-ray diffraction phase analysis indicated that nickel oxalate has been totally reduced to nickel during calcination in the Ar + 10% H_2 atmosphere (Fig. 2). No peaks coming from the nickel oxalate are observed, however the nickel diffraction pattern is shifted towards smaller 2θ angles when compared to the pure nickel standard [25]. The nickel content determined by the Rietveld method was 2.9 wt%, and it was smaller than the target value of 3.6 wt% (1.7 vol.% Ni). Evaluation based on X-ray line broadening delivered a mean nickel crystallite size of 26 nm in the direction perpendicular to the (111) plane. A very small amount of the tetragonal zirconia polymorph (0.9 wt%) has been detected as a result of contamination of the Al/1.7Ni powder with the milling media material.

The amount of nickel measured for the Al/10Ni powder is 21.4 wt%, and it corresponds very well to the target value of 21.82 wt% (10 vol.% Ni). Nickel crystallites showed a size of 30 nm in the direction perpendicular to the (111) plane.

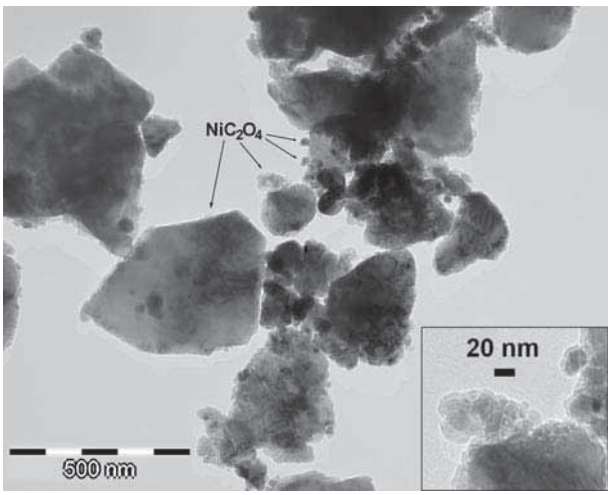

Fig. 1. TEM image of alumina powder with nickel oxalate agglomerates (1.7 vol.% Ni) after milling; an inset shows the detailed morphology of the agglomerate of nickel oxalate nanoparticles jointed to the surface of alumina particle.
Fig. 1. Obraz TEM proszku tlenku glinu zawierającego aglomeraty szczawianu niklu (1,7% obj. Ni) po mieleniu; wstawka pokazuje szczegóły morfologii aglomeratu nanocząstek szczawianu niklu połączonego z powierzchnią cząstki tlenku glinu.

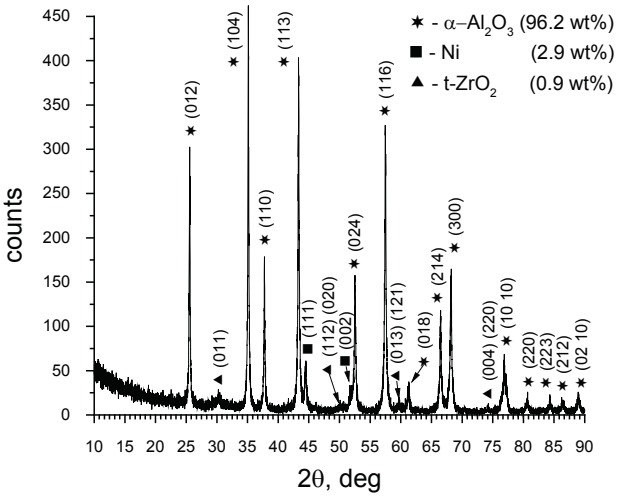

Fig. 2. X-ray diffraction pattern of the alumina powder with 1.7 vol.% Ni (Al/1.7Ni) after nickel oxalate reduction. Peaks coming from nickel oxalate are not detected, and some tetragonal zirconia originating from the 3Y-TZP grinding media is clearly seen.
Rys. 2. Dyfraktogram rentgenowski proszku tlenku glinu zawierającego 1,7% obj. Ni (Al/1.7Ni) po redulcji szczawianu niklu. Widoczny jest brak pików pochodzących od szczawianu niklu oraz obecność tetragonalnego dwutlenku cyrkonu pochodzącego z mielników 3Y-TZP.

3.2. Characteristics of sintered bodies

Phase compositions of the SPS consolidated bodies (Fig. 3) and the initial powders correspond each other in the range of measurement error. The alumina and nickel phase are present in the composites, and the tetragonal polymorph of ZrO_2 is only detected in the Al/1.7Ni composite as the contamination in an amount of 1.5 wt% which corresponds to 1.0 vol.%, assuming the theoretical density of 3 mol% Y_2O_3-ZrO_2 to be 6.1 g/cm^3. The nickel contents of 3.5 wt% (1.6 vol.%) and 22.1 wt% (11.3 vol.%) were determined for

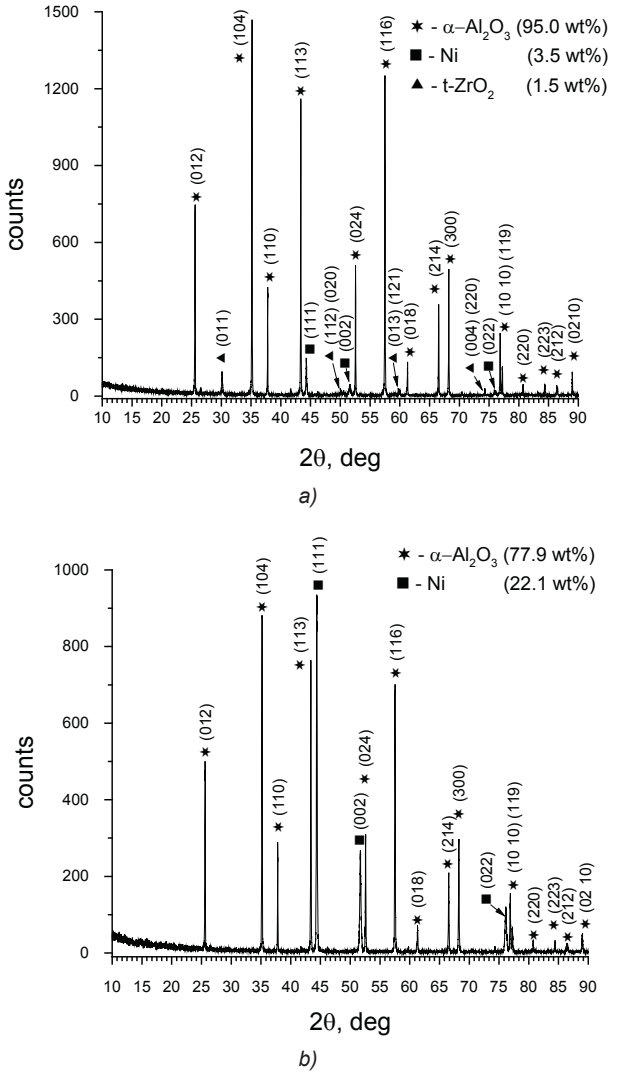

Fig. 3. X-ray diffraction patterns of sintered samples: a) Al/1.7Ni and b) Al/10Ni. The oxalate method allowed the targed values of Ni content to be obtained in the alumina matrix. The attrition milling contaminated the composite with zirconia.
Rys. 3. Dyfraktogramy rentgenowskie spieczonych tworzyw: a) Al/1.7Ni i b) Al/10Ni. Metoda szczawianowa pozwoliła otrzymać założone stężenia Ni w matrycy tlenku glinu. Mielenie atrycyjne wprowadziło do kompozytu zanieczyszczenie tlenkiem cyrkonu.

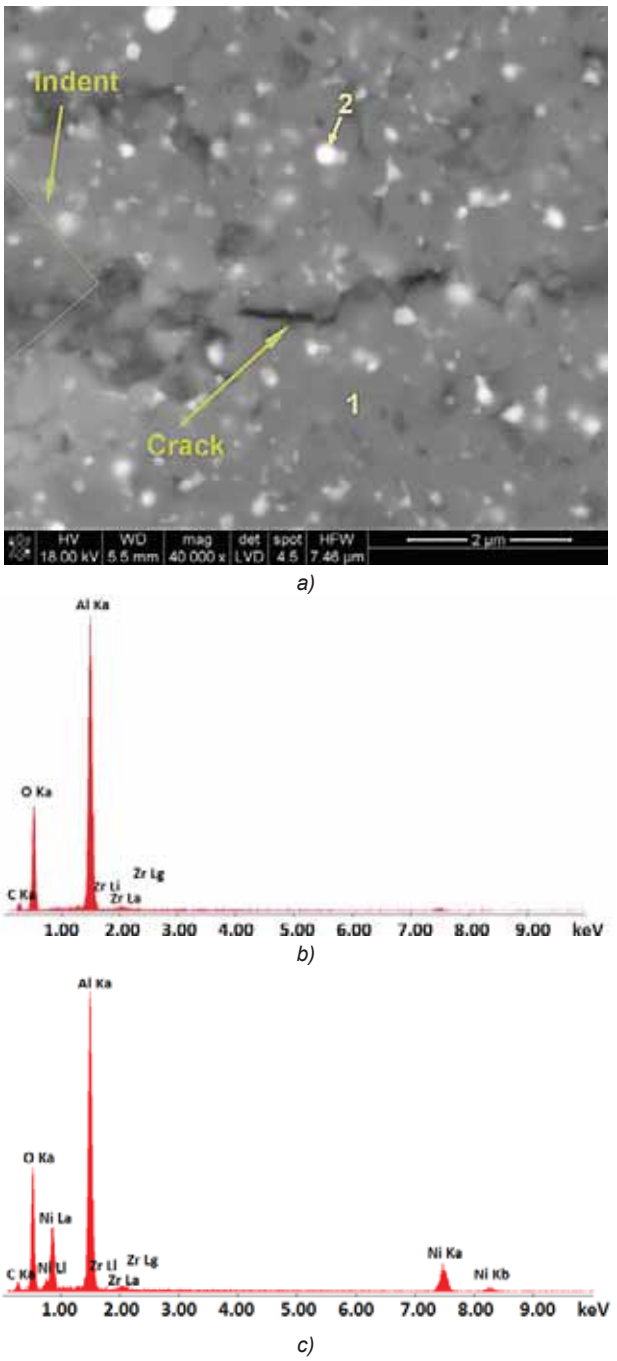

Fig. 4. SEM/EDS studies of the Al/1.7Ni composite: a) micrograph of the microstructure and a crack propagating from an edge of Vickers' indent; the extended surface of fracture is due to the crack deflection mechanism, b) EDS analysis of the alumina matrix (point 1); c) EDS analysis a nickel particle; zirconium is detected in the sample.
Rys. 4. Badania SEM/EDS kompozytu Al/1.7Ni; a) mikrofotografia mikrostruktury z pęknięciem propagującym od naroża odcisku wgłębnika Vickersa; rozwinięta powierzchnia pęknięcia jest spowodowana działaniem mechanizmu odchylania, b) analiza EDS osnowy korundowej (punkt 1), c) analiza EDS cząstki niklu; w próbce wykryto cyrkon.

the Al/1.7Ni and Al/10Ni composites, respectively. There is also a displacement of the X-ray diffraction pattern for the nickel phase of sintered materials when compared to the data of ICSD [25].

The Ni crystallite sizes of 65 nm, 66 nm and 76 nm were determined from X-ray line broadening in the directions perpendicular to the (111), (002) and (022) planes, respectively. In the case of the Al/10Ni composite, the size of 100 nm has been measured by the same method for crystallites of the Ni phase.

The fine-grained microstructure and the satisfactory uniform distribution of nickel nano/microparticles have been obtained for the 1.7 vol.% Ni - alumina composite (Fig. 4a). The largest alumina grains had not the sizes bigger than 1.5 μm, as indicated by some topographic features of the polished section, including the microstructural effects of relief polishing, fracture surfaces in the vicinity of the indent and crack surfaces. Secondary phase particles, that comprised both nickel and zirconia inclusions, had the sizes ranging from 30 nm to 220 nm. EDS measurements permited to reveal that the nickel particles were both spherical and polyhedral in shape (Fig. 4b) and larger in size than the zirconia particles. In the majority of cases the nickel particles showed the sizes close to 130 nm.

The division into two areas occurred in the microstructure of the 10 vol.% Ni – alumina composite (Figs. 5a and 5b). The non-continuous, oval in shape areas (dark parts of

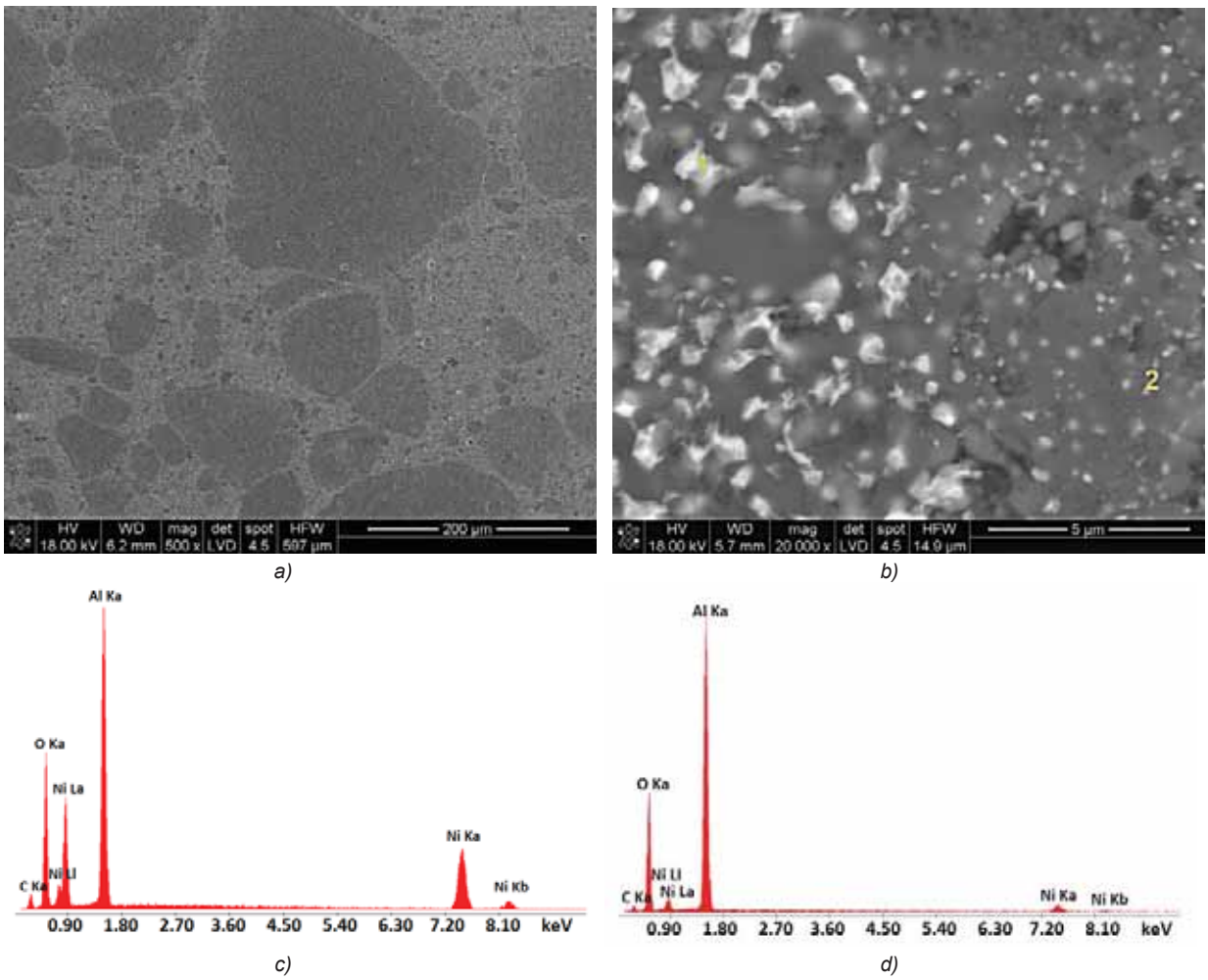

Fig. 5. SEM/EDS studies of the Al/10Ni composite: a) micrograph of the segregated microstructure showing continuous and non-continuous areas, b) boundary zone between continuous and non-continuous areas with marked pointes of the EDS analysis, c) and d) EDS spectra showing Ni contents in continuous and non-continuous areas, respectively. The former area contains more nickel particles than the latter one. Rys. 5. Badania SEM/EDS kompozytu Al/10Ni: a) obraz SEM mikrostruktury rozsegregowanej na obszary ciągły i nieciągłe, b) strefa graniczna pomiędzy obszarami ciągłym i nieciągłym z zaznaczonymi punktami analizy pierwiastkowej, c) i d) widma EDS pokazujące zawartość Ni w obszarach odpowiednio ciągłym i nieciągłym. Ten pierwszy zawiera więcej cząstek Ni.

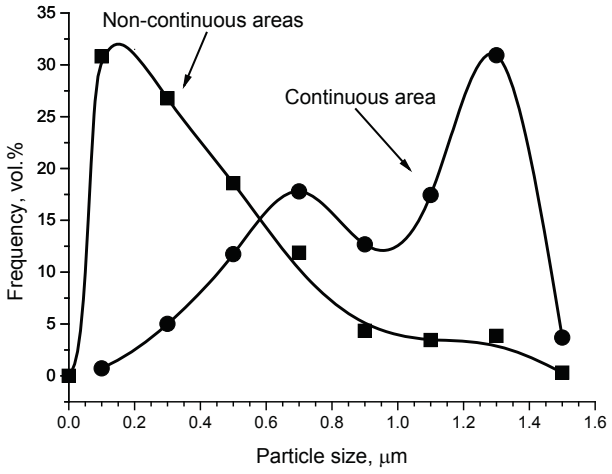

Fig. 6. Size distribution curves of Ni particles for non-continuous and continuous areas detected in the microstructure of Al/10Ni composite.

Rys. 6. Krzywe rozkładu wielkości cząstek Ni w obszarach ciągłym i nieciągłych, wykrytych w mikrostrukturze kompozytu Al/10Ni.

SEM images) were separated by the continuous area (bright parts of SEM images). The non-continuous areas had sizes ranging from a few micrometers to over 300 µm. On the basis of EDS analysis (Figs. 5c and 5d) it was found that the continuous area was richer in nickel particles than the non-continuous one. Quantitative analysis of SEM images indicated about eightfold difference in the Ni concentration (Table 2). The Ni particles were larger in the continuous area (Table 2), and showed a bimodal distribution (Fig. 6). The sizes of Ni particles at the frequency curve maxima (modes) were 1.3 µm / 0.7 µm and 0.15 µm for the continues and non--continuous areas, respectively. The size of alumina grains in both areas showed much smaller diversification than the Ni particles (Table 2). The non-continuous areas showed increased porosity of ~6.5%, but increased hardness values were measured (Table 2) in spite of that.

Alumina polycrystals with no Ni particles (Al/0Ni) showed fine grained microstructures with anisotropy of grain shapes (Fig. 7). Maximum Ferret's diameter of 3.5 µm, maximum length of 4.4 µm and maximum elongation of 3.1 were measured for cross sections of plate-shaped grains.

The increase of density, hardness and fracture toughness was observed for the Ni/alumina composites when compared

Table 2. Characteristics of the continuous and non-continuous areas in the microstructure of Al/10Ni composite.
Tabela 2. Charakterystyki obszarów ciągłego i nieciągłych, wykrytych w mikrostrukturze kompozytu Al/10Ni.

Area	Modal size of Ni particles [μm]	Typical size of alumina grains [μm]	Content of Ni particles [vol.%]	Porosity [%]	Hardness [GPa]
Continuous	1.3/0.7	1.5	25 ± 2	2.0 ± 0.5	13.0 ± 0.6
Non-continuous	0.15	0.9	3.2 ± 0.5	6.5 ± 1.0	16.7 ± 2.0

Table 3. Characteristics of SPS consolidated alumina as a function of Ni content.
Tabela 3. Charakterystyki tworzyw korundowych konsolidowanych metodą SPS jako funkcja zawartości Ni.

Sample	Ni content [vol.%]	Density [%]	Hardness [GPa]	Toughness [MPa/m$^{0.5}$]	Wear resistance [mm^3]
Al/0Ni	0	94.5 ± 0.1	12.2 ± 0.8	4.4 ± 0.3	13.9 ± 0.6
Al/1.7Ni	1.7	96.1 ± 0.1	14.1 ± 0.8	5.8 ± 0.2	3.8 ± 0.4
Al/10Ni	10	95.7 ± 0.1	14.8 ± 1.8*	6.8 ± 0.4	18.8 ± 0.5

**when averaged out for continuous and non-continuous areas of the sample.*

to the pure alumina polycrystal (Table 3) which showed the lowest densification. The largest value of confidence interval calculated for the Al/10Ni composite are directly related to the microstructure segregated on continuous and non-continuous areas, differing in the Ni content.

The best wear resistance showed the Ni/alumina composite containing 1.7 vol.% of the nanometric in size nickel particles (Table 3). The increased content and size of the nickel particles caused the increase in toughness, but simultaneously wear resistance worsened.

4. Discussion

4.1. Preparation of nano-nickel/alumina powders

Production of Ni/Al_2O_3 nano-composites requires the presence of nano-nickel in the composite powder. The oxalate method delivers a nano-precursor for nickel particles, however the oxalate nanoparticles tended to agglomerate, and they were non-uniformly distributed on alumina particles, as observed in the Al/1.7Ni powder (Fig. 1). Drying the oxalate precursor before merging it with the alumina powder favoured the formation of agglomerates, which hindered the homogenization of the nickel oxalate–alumina mixture during the attrition milling and increased both the size of nickel particles obtained during the reduction process, and the size of final nickel particles in the microstructure of sintered composites; the former size is strongly related to the size of the nickel oxalate agglomerates. It thus follows from this discussion that the suspension of as-precipitated nickel oxalate with no drying might be a better starting point for preparation of nano-nickel/alumina composite powders than the dry nickel oxalate powder.

Reductive calcination of the nickel oxalate precursor at 360 °C gave nickel crystallites of ~30 nm in size. There were no growth in crystallite size during the calcination when compared to the size of precursor nickel oxalate particles, as evidenced by this result. A lack of crystallite growth may suggest the unchanged agglomerated structure of the precursor powder after the reductive calcination process.

The nickel particles contained most probably carbon dissolved in solid solution as indicated by a shift of the nickel

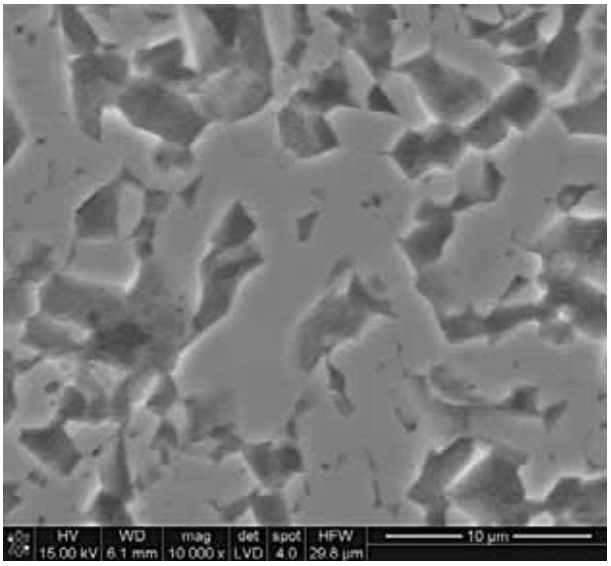

Fig. 7. SEM image of the microstructure of Al/0Ni body. Traces of grains pulled from the surface away indicate an intergranular fracture due to the polyhedral shape, and additionally, facilitates the assessment of grain size on the relief polished surface.
Rys. 7. Obraz SEM mikrostruktury próbki Al/0Ni. Wielościenne ślady ziaren wyrwanych z powierzchni wskazują na przełom międzyziarnowy i dodatkowo ułatwiają ocenę rozmiaru ziaren na powierzchni polerowanej reliefowo.

diffraction patterns towards smaller 2θ angles when compared to pure nickel. If present it affects tensile behaviour and size of nickel particles [26], and may influence the resultant mechanical properties of Ni/alumina composites.

4.2. Microstructural evolution of Ni/alumina composites

The method of incorporation of nickel oxalate particles to alumina power had no influence, in the error of measurement, on the amount of incorporated nickel, as indicated by comparison of the target and measured values of nickel concentrations in the Ni/alumina powders and composites studied. However, it influenced significantly the microstructure of the SPS sintered Ni/alumina composites. The physical mixing of nickel oxalate powder with alumina one assisted

with attrition milling in ethanol delivered the fine-grained microstructure and the satisfactory uniform distribution of nickel nano/microparticles (Al/1.7Ni composite, Fig. 4); however, in the case of direct precipitation of nickel oxalate on alumina particles the division of the microstructure into two areas (continuous and non-continuous) occurred (Al/10Ni composite; Fig. 5). The non-continues areas differed from the continuous one in the content and size of Ni particles, porosity and hardness.

The probable mechanism of evolution of such a microstructure can be related to a local inhomogeneity in distribution of nickel particles within alumina powder, originating from inhomogeneous precipitation of the nickel oxalate crystallites in the presence of alumina particles. The oxalic acid solution has been added dropwise to the suspension of alumina powder containing nickel(II) nitrite during vigorous stirring, and aqueous ammonia adjusted the pH to 4. When precipitating agent (oxalic acid) is added to the solution of nickel ions, it causes a localized excess of the reagent to form in the mixture of solutions. The excess reagent is conducive to rapid formation of a large number of small nickel oxalate crystallites in a form of flocculated (agglomerated) colloid, and promotes non-homogeneities in nickel oxalate distribution in the suspension. Stirring permits to improve uniformity of the nickel oxalate distribution because it increases the motion of nickel oxalate particles in solution and decreases the localized build-up of concentration of ions, equalizing a degree of supersaturation; it therefore slows nucleation and growth of nickel oxalate nanocrystalites, and favours crystallization of larger particles uniform in size. Finally, the alumina particles interact by Van der Waals forces with the nickel oxalate particles, the ions and with each other which can result in hindering the motion of nickel oxalate particles and equalizing ion concentration. This will promote non-homogeneous distribution of the nickel oxalate particles within the alumina powder.

The state of non-uniformity of the nickel oxalate/alumina mixture cannot be changed during the reductive calcination, and the resultant nickel/alumina powder used for the SPS consolidation should contain the areas that differ originally in the nickel content, and therefore they show different electrical conductivities. The passage of an electric current through these areas releases heat in the amount proportional to the square of the current, according to Joule's first law. As a result, the areas of different temperature appear in the material during sintering that densify at different rates, giving the microstructure composed of a continuous area with a high density and nickel content, and low-density, non-continuous areas with a nickel content even smaller then the target value. This microstructural evolution due to differential densification accompanied by the passage of the electric current differs from the microstructural changes induced by differential densification during conventional sintering [27]; reduced densification, increased pore size, radial or circumferential flaws were detected in sinters as a result of structural inhomogeneities in a powder compact.

The observed effects of differential sintering should be attributed not only to the method of incorporation of the nickel particles to the alumina powder, but also to their concentration. Reductive calcination of the physical mixture of nickel oxalate and alumina particles led to the powder containing nickel aggregates non-uniformly dispersed on the alumina particles as suggested by Fig. 1. But the final microstructure of the Al/Ni1.7 composite was uniform (Fig. 4) because the nickel concentration was too low to form paths of high electric conductivity, leading to the microstructural segregation.

The presented results indicate that the Ni/alumina powders for the SPS consolidation should be very homogeneous with respect to the distribution of nickel particles in order to avoid negative microstructural effects of differential densification accompanied by the electric current passage.

Nickel particles inhibited alumina grain growth as predicted by the Zener model [27] (1.5 μm vs. 3.5 μm for the Al/1.7Ni composite and pure alumina grain sizes, respectively), and influenced advantageously densification of the Ni/alumina powder (Table 3).

4.3. Mechanical properties

The mechanism of strengthening in ceramic matrix composites with nanometric metal particles is different when compared to the metal particles of micrometric size [10, 28-29]. In the case of micrometric particles, properties of a composite follow the law of mixtures. So, when soft metal is being introduced into a ceramic matrix, hardness of the resultant material decreases. The mechanism is different, if a size of metal particles, e.g., nickel ones, is smaller than 100 nm and the concentration of the particles is below the threshold of percolation (~15 vol.% for the particles ranging from 20 nm to 100 nm). Accurate control of concentration, spacing and size of the introduced particles is necessary to obtain the effect of hardening which is explained in terms of the Hall-Petch effect [10, 28-31].

The Al/Ni1.7 and Al/10Ni composites obtained by SPS sintering of the nickel oxalate derived composite powders do not fulfil generally the above mentioned requirements for hardening. So, the moderate increase in hardness has been measured. The hardness was additionally affected by porosity, being rather large. However, the non-continuous areas in the Al/10Ni composite contained 3.2 ± 0.5 vol.% nickel particles of 150 nm in size, almost fulfilling the requirements for hardening. In this case the higher hardness of 16.7 ± 2.0 GPa has been measured, suggesting some contribution coming from the Hall-Petch effect.

The addition of nickel particles increased fracture toughness, comparing to the pure alumina polycrystal. The largest values of the critical stress intensity factor, KIc, have been measured for the Al/10Ni composite which showed microstructural segregation of the nickel particles. The continuous area of the composite microstructure contained the amount of Ni increased up to 25 vol.%, and low porosity of 2%, that seem to be responsible for the increased fracture toughness, but decreased abrasive wear resistance. An intergranular fracture was observed in the Al/1.7Ni composite, showing contribution of the crack deflection mechanism to fracture toughness of the composite.

5. Conclusions

A method based on processing nickel oxalate was applied to incorporate nickel nanoparticles to alumina powder.

This method delivers a nano-precursor for nickel particles, however the agglomeration process of the nickel oxalate nanoparticles hinders obtaining nickel nanoparticles in a mixture with alumina particles, and then in a sintered composite. This is a challenge for further studies.

Distribution of the nickel nanoparticles in a starting composite powder is a crucial issue when the powder is SPS consolidated. Inhomogeneities in the nickel particles distribution lead to the microstructural segregation of the nickel phase, being enhanced with the SPS sintering, which affects resultant mechanical properties. A way of incorporation of the nickel precursor to the alumina powder is therefore important. Accurate colloidal processing of nickel oxalate particles seems to have the highest potential for preparation of the alumina powders with homogeneously distributed, non-aggregated nickel nanoparticles.

The Ni/Al_2O_3 composites showed increased hardness, fracture toughness and abrasive resistance when compared to alumina with no nickelic particles. The measured values of hardness were moderate because the sizes of nickel particles slightly exceeded the nanometric limit, and the theoretical density of the composites has not been achieved. The Hall-Petch effect contributed to the hardening of the studied Ni/Al_2O_3 composites in a very limited range.

Acknowledgements

The work was financially supported by the European Union within a framework of European Regional Development Found under Innovative Economy Operating Programme; grant no. POIG.01.03.01-00-024/08. The authors would like to thank Mrs. E. Trybalska and dr. Ł. Zych for their assistance in SEM and BET measurements, respectively. Dr Piotr Putyra from the IZTW - Institute of Advanced Manufacturing Technology is highly appreciated for SPS sintering.

Literature

[1] Tuan, W.H., Brook, R.J.: The toughening of alumina with nickel inclusions, *J. Eur. Ceram. Soc*., 6, (1990), 31–37.
[2] Breval, E., Deng, Z., Chiou, S., Pantano, C.G.: Sol-gel prepared Ni-alumina composite materials, *J. Mater. Sci*., 27, (1992), 1464–1468.
[3] Tuan, W.H., Wu, H.H., Yang, T.J.: The preparation of Al_2O_3/Ni composites by a powder coating technique*, J. Mater. Sci.*, 30, (1995), 855–859.
[4] Sun, X.D., Yeomans, J.A.: Influence of Particle Size Distribution on Ductile-Phase Toughening in Brittle Materials, *J. Am. Ceram. Soc*., 79, (1996), 562–564.
[5] Fahrenholtz, W.G., Ellerby, D.T., Loehman, R.E.: Al_2O_3–Ni Composites with High Strength and Fracture Toughness*, J. Am. Ceram. Soc*., 83, (2000), 1279–80.
[6] Zhu, J.C., Lee, S.Y., Yin, Z.D., Lai, Z.H.: In: Shiota, I., Miyamoto, M.Y. (Eds), *Functionally graded materials*, 1996, Amsterdam: Elsevier Science, 1997, p. 203–208.
[7] Sanchez-Herencia, A.J., Hernandez, N., Moreno, R.: Rheological Behavior and Slip Casting of Al_2O_3–Ni Aqueous Suspensions, J. Am. Ceram. Soc., 89, (2006), 1890–1896.
[8] Konopka, K., Miazga, A., Właszczuk, J.: Fracture toughness of Al_2O_3-Ni composites with nickel aluminate spinel phase $NiAl_2O_4$, *Composites*, 11:3, (2011), 197-201.
[9] Konopka, K., Kuczyński, P., Miazga, A., Riegert, D.: Effect of Sintering Atmosphere on Microstructure and Properties Al_2O_3-Ni Composites, *Materiały Ceramiczne*/*Ceramic Materials*, 64, 1, (2012), 89-93.
[10] Moya, J.S., Lopez-Esteban, S., Pecharromán, C.: The challenge of ceramic/metal microcomposites and nanocomposites, *Prog. Mater. Sci*., 52, 7, (2007), 1017–1090.
[11] Ji, Y., Yeomans, J.A.: Microstructure and Mechanical Properties of Chromium and Chromium/Nickel Particulate Reinforced Alumina Ceramics, *J. Mater. Sci*., 37, 24, (2002), 5229–5236.
[12] Michalski, J., Konopka K., Kurzydłowski K.J., Trzaska, M., Gierlotka, S.: A Possibility to Obtain an Al_2O_3/Ni-P Nanocomposite through Hot Pressing (HP) of Al_2O_3 Powders Covered by Electroless Nickel, *Kompozyty (Composites)*, 3, (2003), 7.
[13] Tuan, W.H., Wu, H.H., Chen, R.Z.: Effect of Sintering Atmosphere on the Mechanical Properties of Ni/Al_2O_3 Composites, *J. Eur. Ceram. Soc*., 17, 5, (1997), 735–41.
[14] Vekinis, G., Sofianopoulos, E., Tomlinson, W.J.: Alumina Toughened with Short Nickel Fibres, *Acta Mater*., 45, 11, (1997), 4651–4661.
[15] Sekino, T., Nakajima, T., Ueda, S., Niihara, K.: Reduction and sintering of a nickel-dispersed-alumina composite and its properties, *J. Am. Ceram. Soc*., 80, (1997), 1139–1148.
[16] Nishimura, Y., Aikawa, K., Choi S.-M., Hashimoto, S., Iwamoto, Y.: Relation between functional properties of alumina-based nanocomposites and locations of dispersed particles, *J. Ceram. Soc. Jpn*, 117, 7, (2009), 836-841.
[17] Zhang, X., Lu, G., Hoffmann, M. J. & Metselaar, R., Properties and interface structures of Ni and Ni-Ti alloy toughened Al_2O_3 ceramic composites. *J. Eur. Ceram. Soc.,* 15 (1995) 225-232.
[18] X. Yao, Z. Huang, L. Chen, D. Jiang, S. Tan, D. Michel, G. Wang, L. Mazerolles, J.-L. Pastol: Alumina–nickel composites densified by spark plasma sintering, *Materials Lett*., 59, 18, (2005), 2314-2318.
[19] Moya, J. S., Rodriguez-Suarez, T., Lopez-Esteban, S., Pecharromán, C., Díaz, L.A.,Torrecillas, R., Nygren**,** M.: Diamond-like Hardening of Alumina/Ni Nanocomposites, *Adv. Eng. Mater.*, 9, 10, (2007), 898–901.
[20] Rodeghiero, E.D., Tse, O.K., Chisake, J., Giannelis, E.P.: Synthesis and Properties of Ni–α-Al_2O_3 Composites via Sol–Gel, *Mater. Sci. Eng. A*, 195, (1995),151–61.
[21] Rodeghiero, E.D, Moore, B.C, Wolkenberg, B.S, Wuthenow, M, Tse, O.K., Giannelis, E.P.: Sol–gel synthesis of ceramic matrix composites, *Mater. Sci. Eng. A*, 244, 1, (1998), 11-21.
[22] Ik-Hyun Oh, Jae-Young Lee, Jae-Kil Han, Hee-Jung Lee, Byong-Taek Lee Microstructural characterization of Al_2O_3–Ni composites prepared by electroless deposition Surface & Coatings Technology 192 (2005) 39–42.
[23] Üstündag, E., Ret, P., Subramanian, R., Dieckmann, R., Sass, S.L.: In Situ Metal–Ceramic Microstructures by Partial Reduction Reactions in the Ni–Al–O System and the Role of ZrO_2, *Mater. Sci. Eng. A*, 195, (1995), 39–50.
[24] Gizowska, M., Konopka, K., Szafran, M.: Alumina Matrix Ceramic-Nickel Composites Wet Processing, *Kompozyty*, 11:1, (2011), 61-65.
[25] ICSD collection code: 41508.
[26] Xiao, C., Mirshams, R.A., Whang, S.H., Yin, W.M.: Tensile behavior and fracture in nickel and carbon doped nanocrystalline nickel, Mat. Sci. Eng., A301, (2001), 35–43.
[27] Rahaman M.N.: Sintering of Ceramics, CRC Press, Taylor &Francis Group, Boca Raton, 2008.
[28] Lopez-Esteban, S., Rodriguez-Suarez, T., Esteban-Betegón, F., Pecharromán C., Moya J. S.: Mechanical properties and interfaces of zirconia/nickel in micro- and nanocomposites, J. Mater. Sci., 41, 16, (2006), 5194-5199.
[29] Esteban-Betegón, F., Lopez-Esteban, S., Requena, J., Pecharromán, C., Moya, J. S.: Obtaining Ni Nanoparticles on 3Y-TZP Powder from Nickel Salts, J. Am. Ceram. Soc., 89, 1, (2006), 144–150.
[30] Rodriguez-Suarez, T., Díaz, L. A., Torrecillas, R., Lopez-Esteban, S., Tuan, W. H., Nygren, M., Moya, J. S.: Alumina/tungsten nanocomposites obtained by Spark Plasma Sintering, Comp. Sci. Tech., 69, (2009), 2467–2473.
[31] Pecharromán, C., Esteban-Betegón, F., Bartolomé, J. F., Richter, G., Moya, J. S.: Theoretical Model of Hardening in Zirconia-Nickel Nanoparticle Composites, Nano Letters, 4, (2004), 747-751.

♦

Received 4 June 2012, accepted 30 October 2012